

**Effects of Electrically-Stimulated Silver-Coated Implants and
Bacterial Contamination in a Canine Radius Fracture Gap Model**

By

Russell Eric Wright, DVM

Thesis submitted to the faculty of the Virginia Polytechnic Institute and State
University in partial fulfillment of the requirement for the degree of

Master of Science

In

Veterinary Medical Sciences

Approved:

Peter K. Shires, Chairman

Jeryl C. Jones

Robert B. Duncan Jr.

July 7, 1999

Blacksburg, Virginia

Key Words: Silver, iontophoresis, radius, fracture, effects, osteomyelitis

Copyright 1999, Russell Eric Wright

Effects of Electrically-Stimulated Silver-Coated Implants and Bacterial Contamination in a Canine Radius Fracture Gap Model

By

Russell Eric Wright

(Abstract)

The purpose of this project was to study the effects of anodic electrically stimulated silver-coated stainless steel implants and bacterial contamination in a canine radius fracture gap model.

Twelve skeletally mature canines weighing 19.2-23.2 kg were used. Dogs were randomly assigned to into control and contaminated groups. A 5 mm ostectomy gap was made in both radii of each dog. One radius of each dog was stabilized with a silver-coated stainless steel bone plate and the other with an uncoated stainless steel bone plate. The ostectomy sites were inoculated with sterile PBS in 6 dogs and *S. intermedius* in the other 6 dogs. Each implant set was electrically stimulated with direct current for 20 minutes daily, for 10 days. Animals were treated with Cephalexin orally for 10 days. Radiographs were obtained at two week intervals. Animals were euthanized at 12 weeks and each plate was cultured. Radiographic, histologic and

bacteriologic evaluations of each radius were performed. The difference in bone healing between silver-coated and stainless steel treated radii was determined for each dog by subjective radiographic evaluation and quantitative analysis of radiographic density using commercial software.

At week 12, a significant decrease in bone healing was found on radiographic evaluations and quantitative bone area analysis of contaminated radii that were treated with electrically stimulated silver-coated implants (p-value 0.025 and 0.018 respectively). Inoculum or implant treatment type showed no significant difference on radiographic evaluations or quantitative bone area analysis. No significant differences were detected in radiographic evaluations of osteomyelitis or histologic evaluations of bone healing, inflammation and peri-implant resorption. Culture results were not indicative of *S. intermedius* inoculated osteomyelitis.

The use of a bilateral radial ostectomy model allowed comparison of electrically-stimulated silver-coated and uncoated implants within each dog. Bone healing in the stable 5 mm fracture gap radial ostectomy model, was progressive in both contaminated and non-contaminated situations. Our study found a negative effect on bone healing when electrically-stimulated silver stearate coated implant were used in *S. intermedius* contaminated radius ostectomies. This trend became apparent at 6 weeks post-operatively, but was not statistically evident until 12 weeks. Further studies are

warranted to evaluate the appropriate protocol, the effects of, and indicated use of this treatment modality in contaminated fractures and clinical osteomyelitis situations.

Grant Information

This project was made possible through the generous financial support of the Virginia Veterinary Medical Association Veterinary Memorial Fund and The AO North America Resident Clinical Trauma Research Program.

Dedication

*I would like to dedicate this manuscript to my loving wife Sarah and our son Caleb,
whose support and understanding were unending and unconditional.*

Acknowledgements

The author wishes to thank Germille Colmano, Martha Moon, Daniel Ward, John Strauss, Taryn Brandt, Susan Ayers, Kim Wright, Jennifer Lesser and Dr. John Robertson for their assistance with this study.

Table of Contents

Abstract	ii
Grant Information	v
Dedication	vi
Acknowledgements	vii
List of Tables	xi
List of Figures	xii
Literature Review	1
Osteomyelitis	1
Implant Associated Infection	4
Pathogenesis of Osteomyelitis	5
Diagnosis of Osteomyelitis	6
Treatment	8
Models of Osteomyelitis	9
Bone Healing	10
Assessment of Bone Healing	11
Models of Bone Healing	13
Medicinal Silver	14
Antibacterial Properties of Silver	15
Silver Toxicity	15
Silver Iontophoresis	16
Clinical Studies	16

Molecular Monolayering	17
Introduction	18
Material and Methods	21
Subjects	21
Silver Coating	21
Bacterial Inoculum	22
Anesthesia and Surgical Procedure	22
Electrical Stimulation	23
Post-operative Monitoring	24
Bone Area Analysis	25
Radiographic Analysis	26
Histologic Analysis	27
Statistical Analysis	28
Results	30
Bone Area Analysis	30
Radiographic Analysis	30
Histologic Analysis	31
Culture Results	32
Discussion	33
Tables	40
Figures	43
References	51

List of Tables

Table 1:	Week 12 Mean Bone Area and Mean Radiographic Bone Healing	47
Table 2:	Mean Difference in Bone Area	48
Table 3:	Mean Difference in Radiographic Bone Healing Scores	49

List of Figures

Figure 1:	Picture of 5 mm Radial Ostectomy Model	50
Figure 2:	Linear Scoring Sheet: Radiographic Analysis	51
Figure 3:	Examples of Radiographic Linear Scoring and Measurement	52
Figure 4:	Linear Scoring Sheet: Histologic Analysis	53
Figure 5:	Examples of Histologic Linear Scoring and Measurement	54
Figure 6:	Image Depicting Bone Area Analysis	55
Figure 7:	Mean Difference in Bone Area	56
Figure 8:	Mean Difference in Radiographic Bone Healing	57

Literature Review

Osteomyelitis is defined in Dorland's Medical Dictionary as inflammation of bone caused by a pyogenic organism.(26) It may remain localized or spread through the bone to involve the marrow, cortex, cancellous tissue, and periosteum. Evidence of osteomyelitis can be found in fossilized creatures dating back 250 million years.(29) In humans, the incidence of osteomyelitis has been reported in the range between 0.5% and 2.7%.(8, 29) While considered rare in dogs, the actual rate of osteomyelitis occurrence has not been reported.

The source of contaminating bacteria in osteomyelitis can be hematogenous, traumatic or iatrogenic in origin. The hematogenous form of osteomyelitis results from bacterial inoculation via the blood stream. It is rarely reported in the dog and cat, but more commonly described in foals, calves, lambs and humans < 16 years of age.(14, 38) The vascular anatomy of the metaphysis in juveniles appears to be the predisposing cause for this form of infection.(14, 29) In juveniles, the nutrient artery enters the diaphysis of long bones and branches proximally and distally. These branches end in nonanastomotic sinusoids beneath the epiphysis. These sinusoids are smaller in diameter than their venous drainage. As a result, turbulent and reduced blood flow occurs at this junction. It has been suggested that infection begins in these sinusoids following bacteremia.(14) This vascular arrangement changes in man with the closure of the growth plate. Therefore, it is uncommon for a hematogenous cause of osteomyelitis to be implicated in adult humans and most other adult animals.

Most cases of osteomyelitis in veterinary medicine are the result of local contamination. Bacterial contamination of bone can occur secondary to open fractures, spread from soft tissue infection, penetrating wounds, or surgical invasion. This is generally classified as posttraumatic osteomyelitis since it is associated with a traumatic event or surgical intervention.(8) Posttraumatic osteomyelitis is a local bone infection and not a systemic condition.

Retrospective studies of canine osteomyelitis have been reported.(14, 76, 82) Cay wood reports that 55% of osteomyelitis cases were associated with open reduction of closed fractures, while only 6% of osteomyelitis cases were attributed to a hematogenous source. Soft tissue extension of infection accounted for 26% and open fractures for 10% of cases.(14) Stead reports that 70% of osteomyelitis cases are related to orthopedic complications, while no incidence of hematogenous osteomyelitis is noted.(82)

Osteomyelitis may be acute or chronic. These two forms of the same disease exhibit different clinical signs depending on the duration of infection. The acute form of osteomyelitis begins post-inoculation. Local signs include soft tissue swelling, pyrexia, pain, reddening of tissues, and lameness.(14, 76, 82) Systemic signs may include pyrexia, anorexia and depression. A complete blood count may demonstrate an elevated white blood cell count and a neutrophilic left shift. The predominant radiographic

finding is soft tissue swelling. These signs are non-specific, making it difficult to distinguish between acute osteomyelitis and post-traumatic inflammation.(29)

The chronic form of osteomyelitis presents primarily as local disease. Systemic signs of pyrexia, anorexia and depression are rarely present. Common clinical complaints include draining fistulous tracts and lameness.(14, 76) Hematological parameters may be within normal limits or demonstrate a mildly elevated white blood cell count with a slight neutrophilic left shift.(14, 76) Radiographic changes may include signs of implant loosening, bone sequestra, sclerosis, osteolysis, soft tissue swelling, and periosteal reaction. Radiographic lesions and clinical signs that persist or are progressive for greater than 4-6 weeks are consistent with a diagnosis of chronic osteomyelitis.

Most cases of osteomyelitis are bacterial in origin. Other etiologic agents such as fungi, parasites, viruses, foreign bodies and metallic implants have been reported.(43, 75, 84, 89) Studies have shown that aerobic and anaerobic, Gram-positive and Gram-negative bacteria have been implicated in osteomyelitis. Caywood and Smith both report a single causative agent in 53% and 59% of cases respectively.(14, 76) *Staphylococcus* spp. are the most commonly isolated organisms from canine osteomyelitis.(14, 76, 82)

Staphylococcus intermedius is the most commonly isolated bacteria of normal canine skin flora.(72) *S. intermedius* was previously identified as *Staphylococcus aureus* until recent nomenclature changes.(13) Studies show that more than half of osteomyelitis cases are related to open reduction of fractures.(14, 76) Stevenson reported a 40% incidence of bacterial contamination, with predominantly *Staphylococcus* spp., in open reduction of closed canine fractures.(83) A study performed at Tulane University found an increase in infection rate of 0.4% to 1.7% when conservatively managed closed fractures were compared to surgically reduced closed fractures.(8) Even with proper aseptic surgical technique, skin contamination during open reduction of fractures is the most commonly implicated source of infection. This explains the high incidence of *Staphylococcus* spp. associated osteomyelitis.

Gristina speculated that biomaterials provided an inert substrate for bacterial growth and propagation.(35) Smith isolated bacteria from 17 of 40 bone plates removed from dogs.(78) Of these cases, 9 were associated with complications such as osteomyelitis and the other 8 showed no clinical or radiographic signs of infection. Petty found an increased rate of infection when canine femurs were inoculated with bacteria and orthopedic implants were used.(61) Implant associated infection can result in a recurrent source of infection that is nonresponsive to antibiotic therapy. Removal of the implant is usually necessary to resolve the clinical signs of infection.

Bacteria produce a slimy glycocalyx that is composed of a matrix of fibrous exopolysaccharides, glycoproteins, or both.(34) The glycocalyx functions to provide adherence, protection and nutrient trapping. The polysaccharides of the glycocalyx are similar in structure to commercial chemical adhesives.(21) This enables bacteria to adhere to biologic implants after contamination during surgery or later from a transient bacteremia. Adhesion properties may be related to bacterial virulence.(34) The thick slime-like coating resists penetration of antibiotics. Furthermore, the glycocalyx protects bacteria from the host's defense mechanisms such as opsonization, surfactants and phagocytosis by macrophages.(34) Once adherent to an implant or foreign body, the glycocalyx forms a biofilm that envelopes microcolonies of bacteria. This physical barrier enables microcolonies of bacteria to resist antibiotic therapy and host defense mechanisms.

Trauma results in hyperemia and inflammation of tissue. Increased capillary permeability allows infiltration with white blood cells. If bacteria are present they can destroy these WBCs resulting in the release of proteolytic enzymes and the formation of purulent exudate.(69) Additionally, hematomas and edema can result in local ischemic pressure necrosis and microvascular stasis promoting tissue death and bacterial colonization.

Once infection has been established, bacterial antigens stimulate macrophages and neutrophils to produce interleukin-1, which attracts additional macrophages, neutrophils

and lymphocytes.(33) Increased production of prostaglandin E2 by these cells results in increased bone resorption. Injection of arachidonic acid, the precursor of prostaglandins, into rat tibias facilitated the formation of osteomyelitis and bone resorption.(67) Models of osteomyelitis use sodium morrhuate, a fish oil derivative containing arachidonic acid, to create bone necrosis and establish osteomyelitis.(58, 70)

As osteomyelitis progresses from the acute to chronic form, it becomes less responsive to antibiotic therapy and host immune response. Inflammatory cells are separated from granulation tissue and a good blood supply by connective tissue which results in bony abscess formation. As the pressure of this purulent exudate increases, it enters cortical bone through the Haversian and Volkmann's canals.(77) Increased porosity of bone secondary to inflammation can lead to subperiosteal elevation and formation of a sequestrum.

Clinical signs and radiographic changes are highly suggestive of posttraumatic osteomyelitis, but confirmation of osteomyelitis is based on identification of an etiological agent. Microbial culture of chronic draining tracts related to osteomyelitis has been shown to be nonrepresentative of the etiologic agent of osteomyelitis.(47) Histologic identification of bacteria was only correct in 33% of osteomyelitis cases.(11) Positive bone cultures are the gold standard for the diagnosis of osteomyelitis. This can be achieved by a surgical approach, fine needle aspirate, or Jamshidi needle biopsy.

Radiographic signs of osteomyelitis vary depending on the duration of disease, subject's age and health, and virulence of the organism. Acutely, the only radiographic evidence that may be seen is soft tissue swelling and decreased delineation of fascial planes in the surrounding soft tissues. Bone resorption is usually not noted initially. Bone demineralization must exceed 35% before it is radiographically evident.(6) Lytic areas may be seen as early as 3 days post-infection in neonates and 5 to 7 days in adults.(69) More commonly, radiographic evidence is first seen 10 to 14 days post contamination. Changes include irregular or interrupted periosteal proliferation, osteolysis, bone sclerosis, implant loosening, increased medullary density, and sequestrum formation. Braden reports that radiographic evaluation of osteomyelitis was 62% sensitive and 57% specific for the diagnosis of experimental osteomyelitis.(11)

Nuclear scintigraphy has been advocated for early diagnosis of osteomyelitis. Technetium-99 pyrophosphate bone scanning has been shown to identify patients with osteomyelitis even before radiographic changes are noted.(87) Unfortunately, this technique has a low sensitivity, particularly in neonates.(87) Indium-111 leukocyte scans were positive one week post inoculation in 83% of rabbits with experimentally-induced osteomyelitis.(64) While scintigraphy may be helpful in the diagnosis of osteomyelitis, a localized increased count can be non-specific for inflammation, trauma, neoplasia and osteomyelitis.

Other imaging modalities can be useful in the diagnosis of osteomyelitis. Computerized tomography (CT) can provide additional information, especially for identifying small foreign bodies as a source of recurrent infection.(29) Magnetic resonance imaging (MRI) can be more sensitive than CT for detecting early osteomyelitis in humans.(16, 28, 40) Diagnostic sensitivities for both modalities are limited by the presence of metallic implants.(29)

Experimentally, enzyme linked immunosorbent assays (ELISA) have been used to detect antibodies to the cell wall of *S. aureus* in animals with concurrent osteomyelitis.(42) Serum IgG concentrations were higher in rabbits with osteomyelitis compared to those with subcutaneous abscesses of the same strain of *S. aureus*. This may prove helpful for identification of osteomyelitis in cases where an etiologic agent can not be identified by standard culturing techniques.(29)

Treatment of osteomyelitis consist of four parts: antibiotics, debridement, drainage and fracture stabilization.(29) Appropriate antibiotic therapy based on culture and sensitivity results is indicated in all cases of osteomyelitis. However, once infection has become established antibiotics alone will not suffice.(8, 29) Surgical debridement of necrotic bone and sequestra is necessary for resolution. Elimination of dead space or surgical drainage must then be established.(8, 29) Finally, stabilization of fractures must be performed when appropriate to eliminate motion that prevents

healing. Bony defects can be treated with cancellous bone grafts to facilitate healing and areas of sclerotic bone should be rongeured to help establish blood supply.(29)

The study of osteomyelitis is mostly dependent on animal models. The earliest attempt to establish a model of osteomyelitis was by Rodet in 1884. This was performed by intravenous injections of a *S. aureus* inoculum into rabbits.(68) Lexer produced bony abscesses in rabbit tibias by intravenous injections of *S. aureus*, but the mortality was high.(45, 46) Other investigators were able to produce suppurative bony lesions with local injections of *S. aureus*, but none of the lesions were progressive.(48, 66) While intravenous and local injection *S. aureus* did produce bony abscesses, these disease models did not accurately reflect the clinical picture of osteomyelitis in humans.

It was not until 1941, when Scheman injected sodium morrhuate into the medullary cavities of rabbit tibias inoculated with *S. aureus*, that a clinically relevant model of progressive chronic osteomyelitis was established.(70) Sodium morrhuate is a sclerosing agent that alone can cause aseptic necrosis of bone.(66) Norden later refined Scheman's protocol to produce the classic model of osteomyelitis in the rabbit tibia. This model consistently produced signs of progressive bony destruction and sequestrum formation.(58) While previous models were unable to produce a progressive form of bone infection, the addition of this sclerosing agent appeared to be the key .

Several canine models have been described. Deysine intravenously injected barium sulfate and *Staphylococcus* spp. into the nutrient tibial artery to establish osteomyelitis.(24) This procedure is technically difficult to perform and the effects of intraarterial barium sulfate are not known.(66) Fitzgerald established osteomyelitis in the canine tibia by inoculating a curretted bone defect with *S. aureus* and filling the defect with a polymethylmethacrylate plug.(27) Petty found that placement of implants in inoculated canine femurs lowered the infection dose necessary to establish osteomyelitis.(61)

Braden reported that an infected wound, avascular bone, and a favorable milieu must be present to establish osteomyelitis in 90% of experimental case of canine osteomyelitis.(8) His model involved trephination of a hole in the canine tibia, traumatization of the medullary canal, inoculation with *S. aureus*, and reinsertion of the bone plug.(9, 10) This established a model of posttraumatic osteomyelitis that did not rely on foreign materials other than the inoculum.

Following fractures, bone healing may be primary or secondary. Primary bone healing relies on rigid stabilization of the fracture and bony contact.(60) Secondary bone healing follows several steps of inflammation, soft callus formation, hard callus formation and bony remodeling.(12) Unlike secondary bone healing, primary bone healing results without the formation of callus. Primary bone healing cannot occur if a fracture gap > 0.1 mm exists.(62)

Following a fracture, disruption of normal blood supply to bone and surrounding soft tissues occurs. Within hours, necrosis of a few millimeters of the fragment ends results from capillary thrombosis in Haversian and Volkmann's canals.(12) Stimulation of afferent vascular components results in increase in diameter and number of vessels.(62) Systemic response to bone injury results in an elevation of parathormone, calcitonin, vitamin D metabolites, and alkaline phosphatase levels.(54) Locally, platelets, mast cells, neutrophils, macrophages, lymphocytes and injured cells within the fracture hematoma release chemoattractants, angiogenic and other growth factors.(12) Platelet-derived growth factor, epidermal growth factor, and transforming growth factor are among those that have been identified.(7, 41, 74) Within a few days, the ingrowth of capillaries serves to engulf the hematoma and macrophages begin to debride the fracture site.(12) Macrophages and neutrophils release interleukin-1 causing muscle atrophy. As a result, these leukocytes and muscle cells increase production of prostaglandin E2 promoting bone resorption.

The soft callus stage begins once inflammation has subsided and ends when fibrous and/or cartilaginous tissue unite the fracture fragment ends.(12) This phase lasts approximately 2-3 weeks leaving the fracture unstable during this process. Osteocytes, periosteal cells and endosteal cells change function to become osteoblasts and chondroblasts. Osteoclasts begin to remove dead bone. Induced osteoprogenitor cells can be found in all connective tissues while determined osteoprogenitor cells can be

found in bone marrow and endosteum.(12) Percutaneous injection of bone marrow has been used experimentally in rabbits as a bone grafting technique.(59)

The hard callus stage occurs as the fracture fragments become united by bone.(12) Mineralization begins between fibrous tissue at the fragment ends and periphery of the callus and spreads towards the center. A front of osteoclasts resorb bone which is followed immediately by new bone deposition. Woven and cancellous-like bone is replaced with lamellar bone. Radiographically and clinically, the fracture appears healed.

The remodeling phase of bone healing can several take years.(12) Once the bridging hard callus is formed, periosteal and endosteal calluses are resorbed. The cancellous cortex of the fracture area is remodeled over time into the normal architecture of Haversian bone.(12)

While clinical and radiographic assessment can determine fracture healing, they are both subjective analyses making comparisons of bone healing in different situations difficult to quantify and document. Progressive radiographic bone healing is defined by gradual mineralization of callus and loss of visualization of the fracture gap.(55) Multiple modalities have been used to quantify bone healing. Dual x-ray absorptiometry (DEXA) is currently one of the standard techniques for measurement of bone mineralization.(51) A dual-energy source is used to quantify differences in

radiographic densities of an object.(51) Quantitative CT and MRI show similar results to DEXA.(49, 50, 52) Quantification of mineral content and density by these DEXA, CT and MRI allows comparison of bone healing in fracture models. These forms of analysis require special equipment to acquire the data. Metallic orthopedic implants cause interference with CT and MRI measurements making them less effective forms of evaluation.

Digital subtraction radiography is a technique for measuring bone density that is currently being used in the field of dentistry.(65) There are reports of its use in angiographic and thoracic studies.(25, 36) The technique involves repeated radiographs over time of the same area of interest. The radiographs are then overlaid and the difference in bone area is measured. This technique is hindered by the need for precise radiographic alignment to produce exact overlays of radiographs for analysis.(65)

The radius provides a good anatomical model for the evaluation of bone healing. Compared to other long bones, there is relatively little soft tissue surrounding the radius. The radius is amenable to multiple forms of stabilization. Bone plating and external skeletal fixation, are appropriate fixation choices for fracture repair. The surgical approach to the bone is simple and less traumatic compared to most other long bones.(62)

Several bone exist for evaluation of healing models in the radius. Millis used a 5 mm radial osteotomy to evaluate the effect of somatotropin on bone healing.(55, 88) This was an unstable fracture model, thus combining the effects of instability and growth factor on fracture healing. Multiple studies evaluating radial osteotomies have been reported.(15, 17, 23) Most were stabilized with external fixation or bone plating. While these studies allow effective testing of the mechanical strength of bone healing, radiographic analysis is more difficult to evaluate due to the lack of a fracture gap. Radius fracture gap models of 2.0 to 2.5 cm in length have are reported.(44, 71) These models are mainly used to evaluate osteoinductive and conductive properties of implants and bone grafting materials. Most controls in these studies progressed to bony non-unions due to the large fracture gap and were not good models of normal fracture healing.

Silver has been long known for its therapeutic qualities.(39) While uncertain of its medicinal uses, silver nitrate was published in a Roman pharmacopeia in 69 B.C. Throughout history, silver has been used to treat multiple illnesses ranging from halitosis to epilepsy. Confirmed medicinal uses of silver were not documented until the eighth century.(39)

Several forms of silver and its salts are currently used for medical therapy.(32) Silver nitrate is a sclerosing agent that is used as a topical chemical cauterizing agent, preventative treatment for gonorrheal ophthalmia neonatorum and wart and corn

removal.(32) Silver sulfadiazine is a combination of silver and a sulfa based antibiotic. It is widely used for the topical treatment of burn wounds.(1, 30) More recently silver-coated urinary and peritoneal dialysis catheters were investigated for the prevention of contamination associated infections.(31) The use of colloidal silver preparations is controversial. It is currently not approved by the United States Food and Drug Administration, but has been advocated as a mineral supplement and an “antibiotic”.(32)

The exact antibacterial mechanism of silver is unknown. Silver readily denatures proteins by binding to their reactive groups, causing precipitation.(32) Silver compounds inactivate enzymes by forming hemisilver sulfides with sulfhydryl groups. Silver can also bind amino, carboxyl, phosphate, and imidazole groups. Shinogi found that silver can diminish the activities of lactate dehydrogenase, glutathione peroxidase, and peroxidation of membrane lipids.(73)

While topical use of silver is relatively safe, chronic ingestion of silver can result in toxic side effects. Known as generalized argyrosis, the classic signs are a greenish-grey or bluish-grey discoloration to the skin and viscera.(53, 63, 86) Toxicity can result in liver and renal dysfunction.(86) Progressive taste and smell disorders, vertigo, hyperesthesia and generalized weakness have also been associated with argyrosis.(86)

The diffusive properties of silver ions from metallic surfaces are poor due to its low solubility in aqueous solutions.(4) Topical silver agents that diffuse more readily, like silver nitrate, are locally sclerosing and toxic in larger amounts. Those silver compounds that are non-toxic, like silver sulfadiazine, poorly dissociate.(39) Anodic electrical stimulation of silver or silver iontophoresis, liberates silver ions allowing diffusion and migration along a voltage gradient. This allows penetration of silver ions into aqueous environments even when structures or tissues are avascular.(4) The silver ions are minimally toxic and at levels far below those necessary to produce an appreciable whole body toxic burden.(4, 39)

Antibacterial effects of silver iontophoresis have been demonstrated both *ex vivo* and *in vivo*.(2, 3, 5, 80) The silver cation has a broad antibacterial spectrum including Gram-positive, Gram-negative, aerobic and anaerobic bacteria with rare reported resistance.(5, 37) Colmano found 100% inhibition of bacterial growth on electrically stimulated intramedullary pins that were coated with 100 monomolecular layers of silver stearate and inoculated with *S. aureus*.(19, 20)

Clinical use of silver iontophoresis for the treatment of osteomyelitis has been reported in three human studies. Becker reported control of bone infection and healing of bony non-unions in 12 of 15 cases using an electrically stimulated intramedullary silver wire or silver nylon dressing.(4) Webster reported resolution of draining tracts in 16 of 25 patients treated with electrically-stimulated silver nylon dressings and 9 of 12

unions of bony non-unions.(85) It should be noted that the patients in both trials were non-responsive to traditional therapy for osteomyelitis. More recently, Nand reported a series of 920 human case of osteomyelitis that were treated with electrically stimulated intramedullary silver wires and electrical osteogenesis. In that series, an 85% control of infection and an 83% resolution of pathologic fractures were reported.(56) These studies showed that silver iontophoresis for the treatment of chronic non-responsive osteomyelitis is promising.

Molecular monolayering of metals involves application of a single molecule thick layer, or multiple layers, of a metal onto the surface of an object.(20) Most metals and their salts can be used to coat an object. Colmano developed a procedure for multiple monomolecular coating of metallic orthopedic implants with silver stearate.(19, 20) By combining this “silver-coating” with silver iontophoresis he was able to inhibit bacterial colonization in rabbit femurs inoculated with *S. aureus*.

Introduction

Contamination of fractures by trauma, surgery and hematogenous sources increases the risk of developing osteomyelitis after surgical stabilization (38, 77). The current treatment for osteomyelitis consists of appropriate antibiotic therapy and surgical debridement. Systemic antibiotics alone have a poor success rate due to the inability to achieve local tissue concentration in areas that have poor vascularity (under orthopedic implants, around foreign bodies, in bony abscesses and in sequestrae). Surgical debridement carries a better prognosis than antibiotic therapy alone and can reach resolution rates as high as 90%, but success is dependent on severity, extent and surgical accessibility (8, 14). The cost of surgical intervention can be prohibitive in veterinary medicine and in human cases in underdeveloped countries (56). Alternative and/or adjuvant non-invasive therapies for the prevention or treatment of osteomyelitis would be useful in both the veterinary and medical communities.

Staphylococcus spp. are the most commonly isolated bacteria in canine osteomyelitis (14, 76). A higher rate of osteomyelitis has been associated with open reduction of fractures (14). This implicates surgical contamination as the leading cause of bacterial contamination (38). *S. intermedius* is the most commonly isolated organism of skin flora in the dog (72). It should be noted that many strains of *S. intermedius* were previously identified as *S. aureus*, specifically those recovered from dogs (13).

Contamination of orthopedic implants increases the risk of chronic infection (61). Poor blood supply, bacterial biofilm or glycocalyx production contribute to a poor response with common modes of therapy (34). Thus surgical removal of implants, foreign bodies or sequestrae is usually necessary to resolve recurrent osteomyelitis infections. Currently there are no additional recommendations for additive therapies to prevent or treat device related infections other than the standard use of appropriate antibiotic therapy and implant removal. Investigation into the use of orthopedic implants coated with antiseptic solutions and silver has shown some success (18, 22).

Silver has been long known for its broad-spectrum antibacterial properties (4, 39, 85). Silver and its compounds have poor tissue penetration and it is usually limited to topical applications. Direct current (anodic) stimulation of silver, or silver ion iontophoresis, liberates silver ions allowing tissue penetration by diffusion and ionic migration along a voltage gradient. Silver ion iontophoresis has experimentally proven antibacterial effects in *ex vivo* and *in vivo* studies (5, 20, 81). Silver ion iontophoresis allows tissue penetration of antibacterial silver ions that is not possible with topical silver preparations.

Cathodic electrical stimulation of silver has shown a favorable osteogenic response and has proven osteogenic activity in healing bone (79). Anodic electrical stimulation may have negative effects on bone healing, but this has not been

documented. While the anti-bacterial effects of anodic stimulation of silver have been proven, the effects on bone healing have not been evaluated.

The use of solid silver implants for orthopedic stabilization is not feasible due to the weak biomechanical properties of silver. Several clinical trials in people have shown favorable results for the treatment of chronic osteomyelitis with silver ion iontophoresis (4, 56, 85). These treatments included intralesional placement of intramedullary silver wire or the use of silver-coated nylon wound dressings. Both methods were invasive and required constant monitoring and care. Colmano found that coating stainless steel intramedullary pins with silver stearate caused 100% inhibition of bacterial contamination in the rabbit femur (20). Silver coating of standard metallic orthopedic implants combines silver ion iontophoresis and proven orthopedic treatment modalities without adding time or trauma to the procedure. The purpose of this study was to evaluate the effects of anodic electrically-stimulated silver-coated stainless steel orthopedic implants that were used to stabilize a contaminated fracture gap model of the canine radius.

Material and Methods:

Subjects: Twelve skeletally mature, non-chondro dystrophoid, mixed breed dogs weighing between 19.2-23.2 kg (mean 20.7 kg) were used. The project was approved by the Virginia Polytechnic Institute and State University Animal Care and Use Committee. Dogs were included in the study if no significant abnormalities were noted on physical examination, complete blood count and differential, biochemistry profile, lameness evaluation, orthopedic examination, and bilateral cranio-caudal and medial-lateral radiographs of the antebrachia.

Silver coating: A surgical stainless steel implant set consisting of a 6-hole, 3.5 mm narrow dynamic compression plate; 6, 3.5 mm cortical bone screws; and a length of 24 gauge orthopedic wire were assigned to each radius of each dog¹. The bone plates were precontoured to the mid-diaphyseal cranial cortex of each radius from medial-lateral radiographs. Screw lengths were similarly selected for the appropriate screw holes. One implant set was randomly chosen for each dog and 100 monomolecular layers of silver stearate were applied.⁽²⁰⁾² Every dog had a stainless steel implant set assigned to one radius and a silver-coated stainless steel implant set assigned to the contralateral radius. All implant sets were gas sterilized prior to surgery. The surgeons and evaluators were blinded to the silver treatment status of each implant set.

¹ Synthes
Paoli, PA 19301-1262

² Colmano Inc.

Bacterial inoculum: A strain *S. intermedius* was isolated from a clinical case of osteomyelitis seen at the Virginia-Maryland Regional College of Veterinary Medicine's Veterinary Teaching Hospital. On the day of each surgery, a sample of the strain of *S. intermedius* was cultured to a concentration of at least 5.0×10^6 CFU per ml (5.6×10^6 to 1.2×10^7 CFU per ml). Six dogs were randomly assigned to receive the inoculum of *S. intermedius* while the other six dogs were assigned to receive a control inoculum of sterile phosphate buffered saline (PBS). The surgeons and evaluators were blinded to the bacterial inoculum status of each subject.

Anesthesia and surgical procedure: Each dog was sedated with acepromazine maleate (0.04 mg/kg of body weight, SC), butorphenol (0.2 mg/kg, SC), and glycopyrrolate (0.02 mg/kg, SC). General anesthesia was induced with thiopental sodium (12 mg/kg, IV). Dogs were intubated, and maintained on inhalant anesthesia with isoflurane. The hair on both forelimbs was clipped and the skin was prepared with povidone iodine and 70% alcohol. Aseptic draping and surgical technique were used.

A standard craniomedial approach to the mid-diaphysis of each radius was performed. The previously assigned bone plate was applied to the cranial mid-diaphyseal region of the radius. The 6, 3.5 mm cortical screws were placed in a neutral position according to standard ASIF technique. The center of the plate was marked on the bone using a #15 scalpel blade, and the screws and plate were removed. A sagittal

saw was used to make a 5 mm radial osteotomy centered at the marked plate center. Using a Stryker drill³, a slightly bent 1.1 mm X 7.5 cm Kirschner wire was inserted into the proximal and distal medullary cavities and allowed to rotate and wobble at full speed for 1 minute per side. The same procedure was performed on the contralateral limb. The medullary cavity and bone of each radius was swabbed for aerobic and anaerobic cultures and a single dose of cefazolin (22 mg/kg, IV) was administered. A 10 X 10 X 7 mm piece of Gelfoam⁴ was placed in the medullary opening of the proximal and distal fragments of each radii. The assigned plate and screws were reapplied to the both radii with the corresponding length of 24 gauge wire anchored under the plate (Fig. 1). The wire exited through a separate skin incision on the medial aspect of the radius. Two tenths of a milliliter, of the randomly assigned inoculum (*S. intermedius* or PBS) was injected into the medullary cavity of the proximal and distal portions of each radius. Both radii in each dog received the same inoculation solution. Routine 3-layer closure was performed with 3-0 polydioxanone suture material.

Electrical stimulation: A 22 gauge needle was inserted into the subcutaneous tissue of the dorsal interscapular region and used as a negative ground electrode. A positive electrode was attached to the 24 gauge plate wire. Beginning immediately post-operatively, 25 microamperes of direct current was applied to each set of bone plates

³ Stryker
4100 East Milham Ave.
Kalamazoo, Michigan 49001
⁴ Pharmacia & Upjohn Company
Kalamazoo, MI 49001

and screws for 20 minutes daily for a total of 10 treatments. After the last treatment, the wire and skin was prepared with povidone iodine and the wire was cut short. The wire exit wound was closed with a single skin staple.

Post-operative monitoring: Medial-lateral radiographs were performed on each radius post-operatively and at 2 week intervals for a total of twelve weeks. An aluminum combination step wedge⁵ was included in each radiograph as a radiographic density control. The same radiographic cassette, technique and positioning were used for each evaluation. Butorphenol (0.4 mg/kg, SQ TID) was administered during the initial post-operative period (24 hours) for analgesia. Acetaminophen with codeine (2 mg/kg, PO TID based on the codeine dosage) was administered for an additional 4 days. Cephalexin (22 mg/kg, PO TID) was administered for 10 days post-surgery. The animals were monitored daily for signs of morbidity and lameness. Additional analgesics were provided, if necessary.

At the end of the 12 week study, each subject was euthanized with an intravenous overdose of pentobarbital-sodium. The hair on both forelimbs was clipped and the skin was prepped with povidone iodine and 70% alcohol. Observing aseptic technique, a cranial incision was made over the length of each bone plate. Aerobic and anaerobic swab cultures of the osteotomy areas were performed.

⁵ Combination step wedge and spin top
Model #455
Harry B Rusk Inc.

Bone area analysis: All radiographs were scanned to create digital images using a VXR-12 film digitizer⁶. Bone area analysis was performed on a Macintosh computer using public domain NIH Image software program Version 1.61⁷. The area of analysis was defined as the area bordered by the bone plate, the trans-cortex, and the 3rd and 4th screws on medial-lateral radiographs (Fig. 4). The average pixel density of the first step of the stepwedge was assigned as the low threshold density value. The pixel density of the bone plate and screws was used as the high threshold. Bone area (BA) was determined as a percentage of the area of analysis and was calculated as follows:

$$\text{Bone Area} = \frac{\text{\# pixels within area of analysis whose density is between upper and lower thresholds}}{\text{Total \# of pixels within the area of analysis}} \times 100$$

The BA was calculated at each evaluation according to treatment (silver or stainless steel) and inoculum (control or contaminated) of each radius. The difference in bone area (DBA) was calculated for each dog at each evaluation as the BA of silver treated radius minus the BA of stainless steel treated radius.

Wichita, KS 67214

⁶ VIDAR Systems Corporation
460 Spring Park Place
Herndon, VA 20170

⁷ U.S. National Institute of Health
<http://rsb.info.nih.gov/nih-image/>

Radiographic analysis: Radiographs were evaluated on two separate occasions by the consensus of 2 reviewers (JCJ, MM). Both reviewers were blinded to the silver treatment and bacterial inoculum status of each radius and dog. Each radiograph was subjectively assessed for two criteria: bone healing and osteomyelitis. A 12 cm linear scale with 2 anchor points was used to score bone healing (Fig. 2 & 3). The first anchor point, “fracture gap”, was placed at the 3 cm mark and defined as the area devoid of continuous bone on immediate post-operative medial-lateral radiographs. Radiographic evidence of bone resorption (widening of the fracture gap) could be documented by placing a mark to the left of the fracture gap anchor point. The second anchor point, “healed”, was placed at the 12 cm mark and defined as continuous bone between proximal and distal radius with visible fracture gap. Linear scoring marks were measured from the 0 cm mark to the reviewers mark and recorded as the radiographic bone healing (RBH) score. The difference in radiographic bone healing (DRBH) was calculated for each dog at each evaluation as the RBH of silver treated radius less the RBH of stainless steel treated radius.

A 12 cm linear scale with 2 anchor points was also used to score radiographic signs of osteomyelitis (Fig. 2 & 3). Radiographic signs of osteomyelitis were defined as radiographic evidence of periosteal proliferation, soft tissue reaction, implant loosening, osteolysis and delayed/non-union. The first anchor, “none”, was placed at the 0 mark and defined as no radiographic signs of osteomyelitis. The second anchor point,

“severe”, was placed at the 12 cm mark and defined as severe radiographic signs of osteomyelitis. Linear scoring marks were measured from the 0 cm mark to the reviewers mark and recorded .

Histologic analysis: At necropsy, each radius was isolated and bone plates and screws were removed. Each radius was bisected longitudinally through the screw holes with the saw blade oriented in the same direction as the screw holes. The samples were fixed in 10% neutral buffered formalin. A 2 mm thick longitudinal slice of the radial diaphysis containing the area of the fracture gap and screw holes was obtained. Each specimen was decalcified in TBD-2 (26.0 % formic acid, 8.5% sodium citrate)⁸, processed routinely, paraffin embedded, sectioned at 5 μ m, and stained with hematoxylin and eosin.

All specimens were evaluated by one pathologist (RBD) who was blinded to the silver treatment and bacterial inoculum status of each radius and dog. Specimens were graded for bone healing and inflammation (severity and type). Bone healing was graded on a 5 point scale based on morphology characteristics of healing (Fig 4 & 5). These points were “no union”, “fibrous union”, “osteochondral union”, “bony union”, and “reorganization of bone”. Inflammation was evaluated in 3 areas (medullary, cortical and peri-implant) by two characteristics (severity and type) (Fig 4 & 5). Severity of

⁸ Shandon-Lipshaw
Pittsburg, PA 15275

inflammation was evaluated on a 12 cm linear scale with 2 anchor points. The anchor “none” was placed at the 0 cm mark and defined as no histologic signs of inflammation. The anchor “severe” was placed at the 12 cm mark and defined as severe histologic signs of inflammation. Type of inflammation graded as the predominant cellular response (fibrous tissue, monocytic, lymphocytic/plasmocytic, and suppurative). Peri-implant bone resorption was measured on a 12 cm linear scale with 2 anchor points (Fig. 4 & 5). The anchor “none” was placed at the 0 cm mark and defined as no signs of peri-implant bone resorption. The anchor “severe” was placed at the 12 cm mark and defined as severe peri-implant bone resorption seen as osteoclasts. Linear scoring marks were measured and recorded.

Statistical analysis: The experimental design was a split-split-plot with inoculum as the whole-plot, implant type as the sub-plot and evaluations as the sub-sub-plots. The BA and RBH values were separated by implant treatment (silver-coated or stainless steel) and inoculum group (control or contaminated). The DBA and DRBH values were separated by inoculum group (control or contaminated). Values were analyzed by repeated measures ANOVA using the MIXED procedure of SAS (version 6.12) software⁹. Significant interactions were further analyzed using the SLICE option to compare levels of one factor (i.e. contamination) within each level of another factor (i.e. evaluations). Histologic analysis of bone healing, inflammation, and peri-

⁹ SAS Institute Inc.
Cary, NC 27513

implant bone resorption between legs of each dog were analyzed by ANOVA using the MIXED procedure. Histologic grading of the type of inflammation was analyzed by Chi-squared analysis.

Results:

One dog was removed from the study after a non-displaced ulnar fracture was detected on radiographs taken 3 weeks post-operatively. The dog was in the contaminated group and the fracture occurred on the leg stabilized with silver-coated implants. No underlying cause was determined for the fracture. The data from a total of 5 contaminated and 6 control dogs were used for analysis.

Bone area analysis: Bone area (BA) evaluations by implant treatment and inoculum showed no statistically significant difference between groups (Table 1). Initial Difference in bone area (DBA) evaluations showed no statistical difference between control and contaminated groups (Table 2). At week 6, the DBA evaluations of the control and contaminated groups began to diverge (Fig. 7). An increasing trend in the DBA for the control group and a decreasing trend for the contaminated group were observed. At week 12, a significant difference was noted between the DBA evaluations of the control (mean 9.10 +/- 6.60%) and contaminated groups (mean -14.89 +/- 7.23%, p-value = 0.018) (Table 2).

Radiographic analysis: Radiographic bone healing (RBH) scores by implant treatment and inoculum showed no statistically significant difference between groups (Table 1). Initial Difference in radiographic bone healing (DRBH) scores showed no statistical difference between control and contaminated groups (Table 3). At week 8 the DRBH scores of the control and contaminated groups began to diverge (Fig. 8). An

increasing trend in DRBH for the control group and a decreasing trend for the contaminated group were observed. By week 12, a significant difference was noted between the DRBH scores for the control (mean 1.69 +/- 1.06 points) and contaminated groups (mean -1.97 +/- 1.16 points, p-value=0.025) (Table 3).

Radiographic scoring evaluations showed no significant signs of osteomyelitis over the entire study in any treatment group (control/stainless steel mean score 0.1 points, control/silver mean score 0.1 points, contaminated/stainless steel mean score 0.3 points, contaminated/silver mean score 0.2 points). Therefore, no significant differences were noted between inoculum groups or implant treatments over time for radiographic analysis of osteomyelitis.

Of the 22 radial osteotomies evaluated, 19 showed radiographic evidence of progressive healing by week 12. The remaining 3 radii had radiographic signs of atrophic non-union. Two of these radii were within the same dog; the other was in the control group and treated with stainless steel implants.

Histologic analysis: Histologic evaluation of bone healing showed no significant difference in bone healing between groups or treatments. The histologic bone healing score was similar for both groups of stainless steel treated radii (control group mean score 6.0 points, contaminated group mean score 5.9 points). Histologic scoring of bone healing were higher for control group silver-treated radii (mean score 7.2 points) and

lower for contaminated group silver-treated radii (mean score 4.1 points) when compared to stainless steel treated radii of control and contaminated groups.

Histologic scoring evaluations of inflammation showed no significant differences between inoculum groups or implant treatments in peri-implant, cortical or medullary bone. Peri-implant inflammation scores were higher for control radii (stainless steel mean score 2.3 points, silver mean score 2.6 points) than for contaminated radii (stainless steel mean score 1.7 points, silver mean score 1.3 points). Five radii showed medullary inflammation (3 control, 2 contaminated) and 3 showed cortical inflammation (2 control, 1 contaminated). No bacteria were noted histologically.

Culture results: No significant growth was noted on intra-operative aerobic and anaerobic intra-operative cultures obtained prior to inoculation. Pathogens cultured at necropsy were not consistent with the inoculum status of each radius. The 3 radii that cultured positive for *S. intermedius* were in the control group. Three radii cultured other bacteria pathogens (*Corynebacterium* sp. & *Pasteurella* sp., *Enterococcus* sp., *Streptococcus* sp.)

Discussion:

Several models of fracture healing in the radius have been reported in the dog. A 2.0-2.5 cm stabilized radial osteotomy is most commonly used to evaluate bone osteogenic and osteoconductive treatments. Untreated controls in these models progressed towards atrophic non-union. Radial osteotomy models do not provide an adequate fracture gap to evaluate bone healing ingrowth on radiographs and are more commonly used for mechanical analysis of fracture healing. A fracture gap of 5 mm was chosen for this model to allow evaluation of radiographic bone healing over time for comparison between treatment groups. Our model showed progression of bone healing in 19 of 22 radius osteotomy sites. Of the 3 radii that were progressing towards atrophic non-union, 2 of these were noted in the same dog and were attributed to biologic variation between subjects. The other non-union was in contrast to the opposite silver-coated implant treated control leg that had healed by week 12. These differences were responsible for the higher BA and RBH seen in the control silver coated implant treated group (Table 1). No cause for the difference in healing between the legs could be determined.

We chose a bilateral radial osteotomy model to allow comparison of implant treatments between legs of the same dog. Although the BA and RBH scores suggest a difference between treatments, no statistical significant difference was found (Table 1). This could be due to the small sample size. Comparison of implant treatments between legs of each dog showed a significant difference between DBA and DRBH at week 12

radiographic evaluations. Comparing treatments between legs of each dog corrected for errors associated with biologic variation.

Culture results were not indicative of osteomyelitis nor did they correlate with the inoculum status of each subject. Definitive diagnosis of osteomyelitis is made with culture results or histologic identification of bacteria (11). The radii from which *S. intermedius* was cultured were in the control group. The other bacterial pathogens identified were different from the *S. intermedius* inoculum. Single rather than multiple pathogens are commonly implicated in osteomyelitis (14, 76). No significant signs of osteomyelitis were noted on radiographic evaluations and no significant differences were noted between control or contaminated radii on histologic evaluation of inflammation. Therefore our culture results may have been due to contamination at the time of culturing or ascending contamination via the exit wound of the implant electrode.

Silver has been long known for its broad-spectrum antibacterial properties (4, 39, 85). Silver nitrate has been used as a topical antibacterial and cauterizing agent, but has fallen out of favor with the discovery of antibiotics. Silver sulfadiazine is currently used as a topical antibacterial, specifically in human burn patients. Human medical research has recently focused on the use of silver impregnated urinary catheters for the prevention of catheter related urinary tract infections.

Electrode implantation and cathodic electrical stimulation of silver electrodes has created a favorable osteogenic response (79). Direct current (anodic) stimulation or silver ion iontophoresis has proven broad-spectrum antibacterial effects (5, 20, 81). The underlying mechanism of anodic silver antibacterial properties is still unknown. Silver and its compounds have poor tissue penetration to exploit their antibacterial properties without precipitating toxic side effects (4, 85). Silver ion iontophoresis liberates silver ions allowing deeper tissue penetration by diffusion and ionic migration along a voltage gradient. This allows tissue concentrations of silver ions that could not be achieved with topical application alone.

Few studies of the treatment of bacterial osteomyelitis with silver ion iontophoresis have been reported. Becker and Webster reported human clinical trials with adjuvant treatment of chronic osteomyelitis associated bony non-unions (4, 85). They reported bony healing in 12 of 15 treated with intramedullary silver wire and 9 of 12 treated with silver-coated nylon dressings respectively. Nand reported 85% resolution of osteomyelitis and 83% healing of septic non-unions in a case series of 920 human osteomyelitis patients treated with intramedullary anodic silver wire (56). Both Becker and Nand reversed polarity of the electrical stimulation for the cathodic osteogenic benefits of silver. While these studies show favorable benefits, the multiple treatment modalities used and the lack of control subjects makes it difficult to evaluate the direct effects of anodic electrical stimulation of silver on bone healing.

While studies have evaluated the antibacterial effects of anodic electrical stimulation of silver, no study has compared the effects of this treatment modality on bone healing. Our study allowed comparison between clean and *S. intermedius* contaminated radial fracture gaps treated with anodic electrically stimulated stainless steel and silver stearate coated stainless steel bone implants within each dog. Anodic electrical stimulation of silver may have temporarily had an overall negative effect on bone healing. A bone healing control group would be necessary to document this effect. Electrically-stimulated, contaminated, silver-coated stainless steel implant treated radii had less bone healing at the end of the study when compared to the contralateral, contaminated, stainless steel implant treated radii. The underlying mechanism of this interaction of *S. intermedius* contamination and anodic electrical stimulation of silver remains unclear.

Silver-coating of orthopedic implants allows the possibility of adjuvant treatment for orthopedic infection using silver ion iontophoresis. Our results showed that silver stearate coated implants that were electrically stimulated for 10 daily, 20 minute treatments and contaminated with *S. intermedius* decreased the amount of bone healing over time when compared to control dogs. Prophylactic treatment of contaminated fractures with this treatment protocol alone cannot be justified by our findings. However, the antibacterial benefits of silver ion iontophoresis may still be helpful in the treatment of osteomyelitis. Further investigation is necessary to determine the effects

of different types and dose of electrical stimulation, positioning of electrodes, silver iontophoresis on local tissues, and implications of using different bacterial strains.

Mineralization of callus is a direct indicator of radiographic bone healing (55). Computer software analysis of radiographs allowed quantification of bone healing by converting radiographic images into digitized pictures made up of pixels based on a scale of gray. The combination stepwedge in each radiograph provided a low density threshold control, while the bone plate and screws were used as a high density threshold. As radiographic mineral content increased, increased number of pixels between the two thresholds were noted in the area of analysis. Bone area analysis and radiographic evaluations showed similar trends and results (Figs. 7 & 8).

Digital analysis of radiographs offers a promising quantitative alternative to subjective radiographic evaluation of bone healing. Like most subjective analysis, radiographic evaluation of bone healing lends itself to evaluator variation and bias. Quantitative, non-subjective techniques have been developed to evaluate bone healing (57, 65, 88). Subtraction radiography uses baseline radiographs and compares them to subsequent radiographic overlays to evaluate new bone formation. It is limited by the precise radiographic positioning that allows comparison between radiographs and is used mainly for dental radiography (65). While similar in concept to subtraction radiography, our technique measured a percentage of bone within a defined area reducing the error associated slight variations in positioning. This allowed quantitative

comparison between radiographs without the need for precise radiographic overlays. Dual x-ray absorptiometry, radionuclide analysis and computed tomography are also currently used to measure bone density (55, 57, 88). These methods require additional cost and specialized equipment that is not available in most clinical settings. The combination stepwedge is inexpensive and the software used is public domain. Our process is only cost limited by the use of a radiographic scanner. Radiographs can be evaluated by this process *ex situ* if a scanner is not available. Our technique of digital analysis of bone area was both affordable and practical. Results paralleled those of subjective evaluations and reached similar conclusions. Further studies to validate this technique are warranted.

A model of post-traumatic osteomyelitis in the canine radius has not been established. Our study was unable to verify the presence of the inoculated bacteria on cultures or cytology. Braden established osteomyelitis in the canine tibia by trephination and devascularization of the medullary cavity with a spinning K-wire (9). We adapted this model to the radius in order to assess the effects of electrically stimulated silver-coated implants. *S. intermedius* was chosen because it is the most commonly isolated bacterium in osteomyelitis (14, 76). Our initial trials showed severe radiographic and clinical signs of osteomyelitis. Several contaminants were noted as well. Antibiotics were added to the treatment regimen in order to reduce morbidity, ascending contamination via the exit wound of the implant electrode, and to simulate the clinical treatment protocol commonly used for open reduction of contaminated

fractures. The addition of antibiotics to our model effectively eliminated clinical, radiographic and bacteriological signs of osteomyelitis. Elimination or modification of our antibiotics protocol may be effective in establishing a clinically apparent fracture gap model of post-traumatic osteomyelitis in the canine radius. Further investigation would be necessary to establish this model.

Conclusion: Bone healing in the stable 5 mm fracture gap model of the radius, was progressive in 19 of 22 contaminated and non-contaminated situations. Anodic electrically stimulated silver-coated implants had a positive effect on bone healing in the non-contaminated and a negative effect in the contaminated group. Further studies are warranted to evaluate the appropriate protocol, the effects of, and indicated use of this treatment modality in contaminated fractures and clinical osteomyelitis situations.

Table 1

Bone Area and Radiographic Bone Healing at Week 12

Group	BA +/- Std	RBH +/- Std
Control & Stainless Steel	79.56 +/- 22.05 %	8.88 +/- 3.56 pts
Control & Silver	88.66 +/- 12.35 %	10.58 +/- 1.43 pts
Contaminated & Stainless Steel	79.83 +/- 27.04 %	8.17 +/- 4.07 pts
Contaminated & Silver	64.94 +/- 30.14 %	6.21 +/- 4.02 pts

Week 12 Mean Bone Area (BA) and Mean Radiographic Bone Healing (RBH) evaluations of radius fractures with standard deviations separated by inoculum (control & contaminated) and implant treatment (silver-coated and stainless steel).

Table 2

Mean Difference in Bone Area

% Difference in Bone Area (DBA)							
Week	0	2	4	6	8	10	12
Control (+/- 6.60 %)	3.59	-5.73	-2.48	4.84	9.29	8.49	9.10
Contaminated (+/- 7.23 %)	-1.45	0.05	-1.03	-3.07	-6.86	-10.68	-14.89
P-value	0.61	0.56	0.88	0.42	0.10	0.06	0.02

Mean Difference in Bone Area (DBA) values with standard error and P-value over time.

Table 3

Mean Difference in Radiographic Bone Healing

Difference in Radiographic Bone Healing (pts)							
Week	0	2	4	6	8	10	12
Control (+/- 1.06 pts)	0.00	-0.11	0.26	0.53	1.72	1.66	1.69
Contaminated (+/- 1.16 pts)	0.00	0.14	0.24	0.42	-0.29	-1.32	-1.97
P-value	0.61	0.87	0.99	0.94	0.21	0.06	0.02

Mean Difference in Radiographic Bone Healing (DRBH) scores with standard error and p-values over time.

Figure 1.



Model of a 5 mm ostectomy of the radius stabilized with 6-hole stainless steel bone plate and screws with a 24 gauge wire electrode placed under plate.

Figure 2: Radiographic Evaluation Sheet

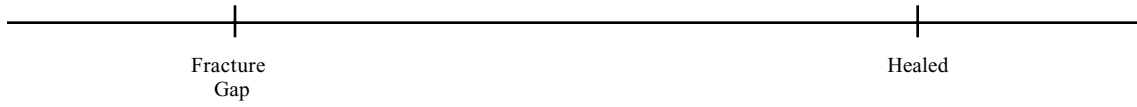
Dog # ____

Week ____

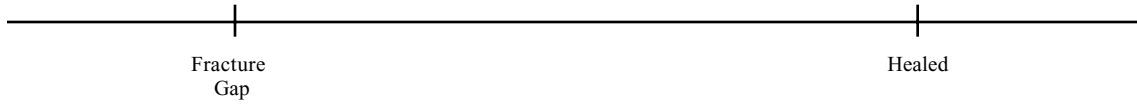
Evaluation ____

Bone Healing

Left

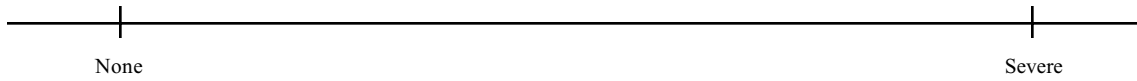


Right



Osteomyelitis

Left



Right

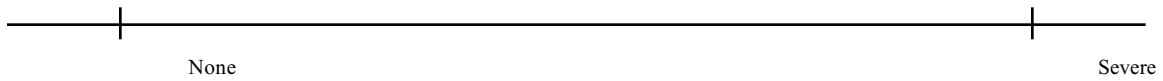


Figure 3: Examples of Radiographic Linear Scoring and Measurement

Dog # ____ Week ____ Evaluation ____

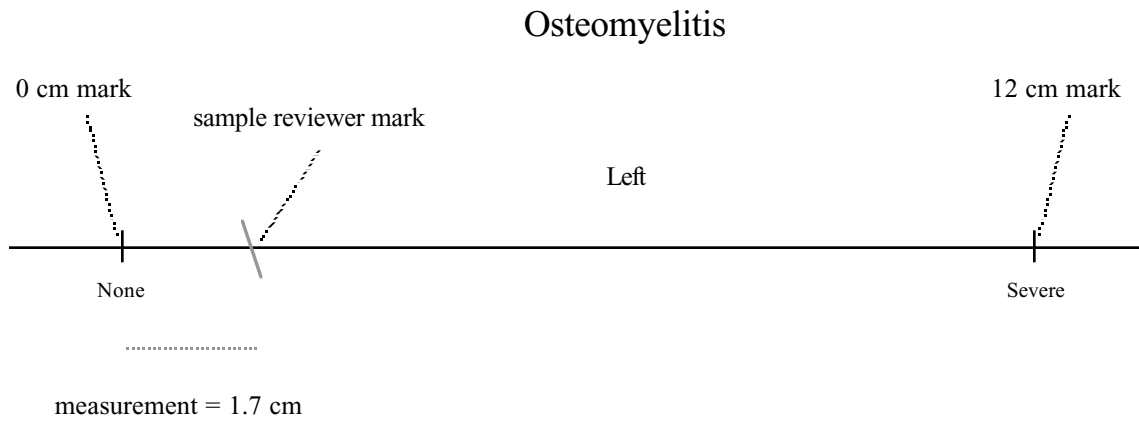
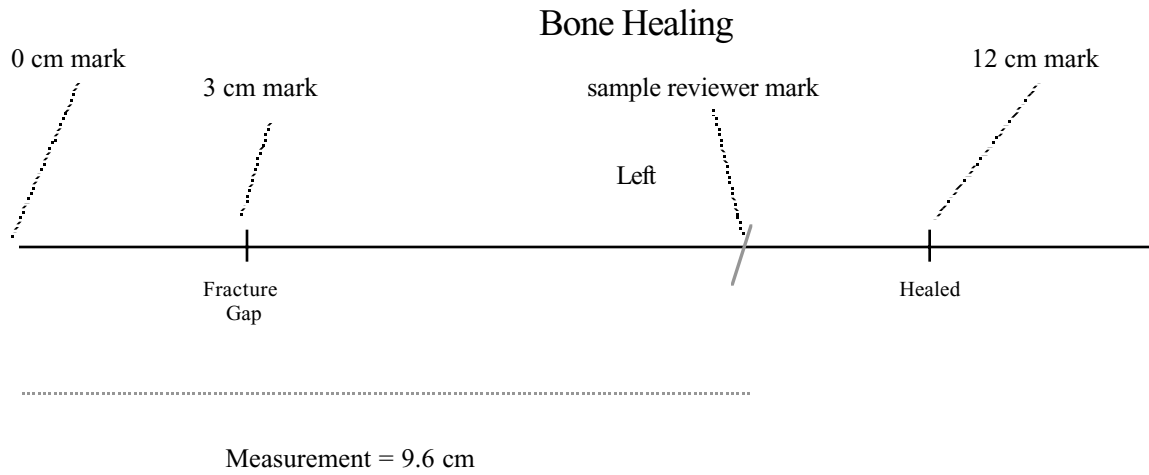
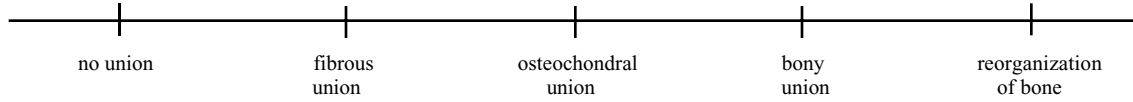


Figure 4: Histology Evaluation Sheet

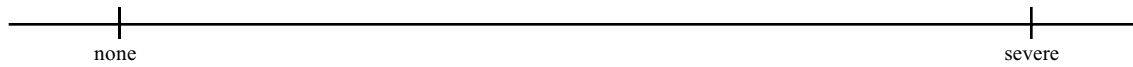
Leg _____
Dog # _____

Bone Healing

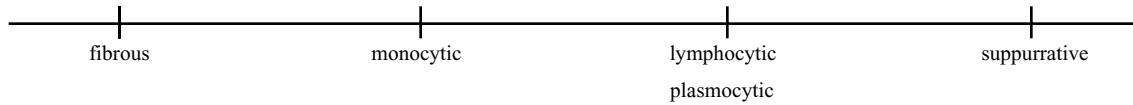


Inflammation

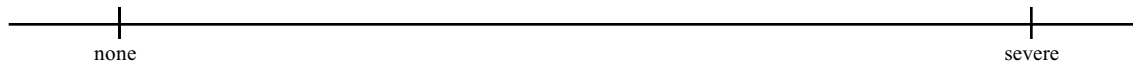
Severity: Medullary



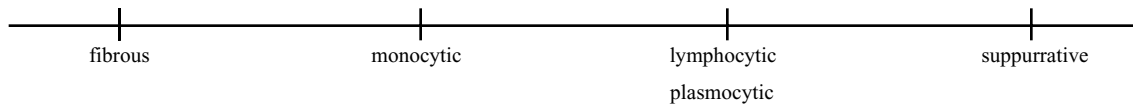
Type: Medullary



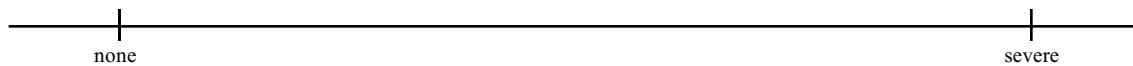
Severity: Cortical



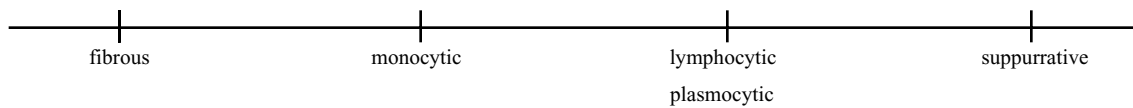
Type: Cortical



Severity: Peri-implant



Type: Peri-implant



Peri-implant Bone Resorbption

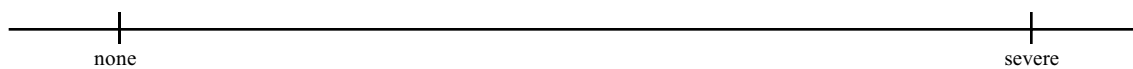


Figure 5: Examples of Histologic Linear Scoring and Measurement

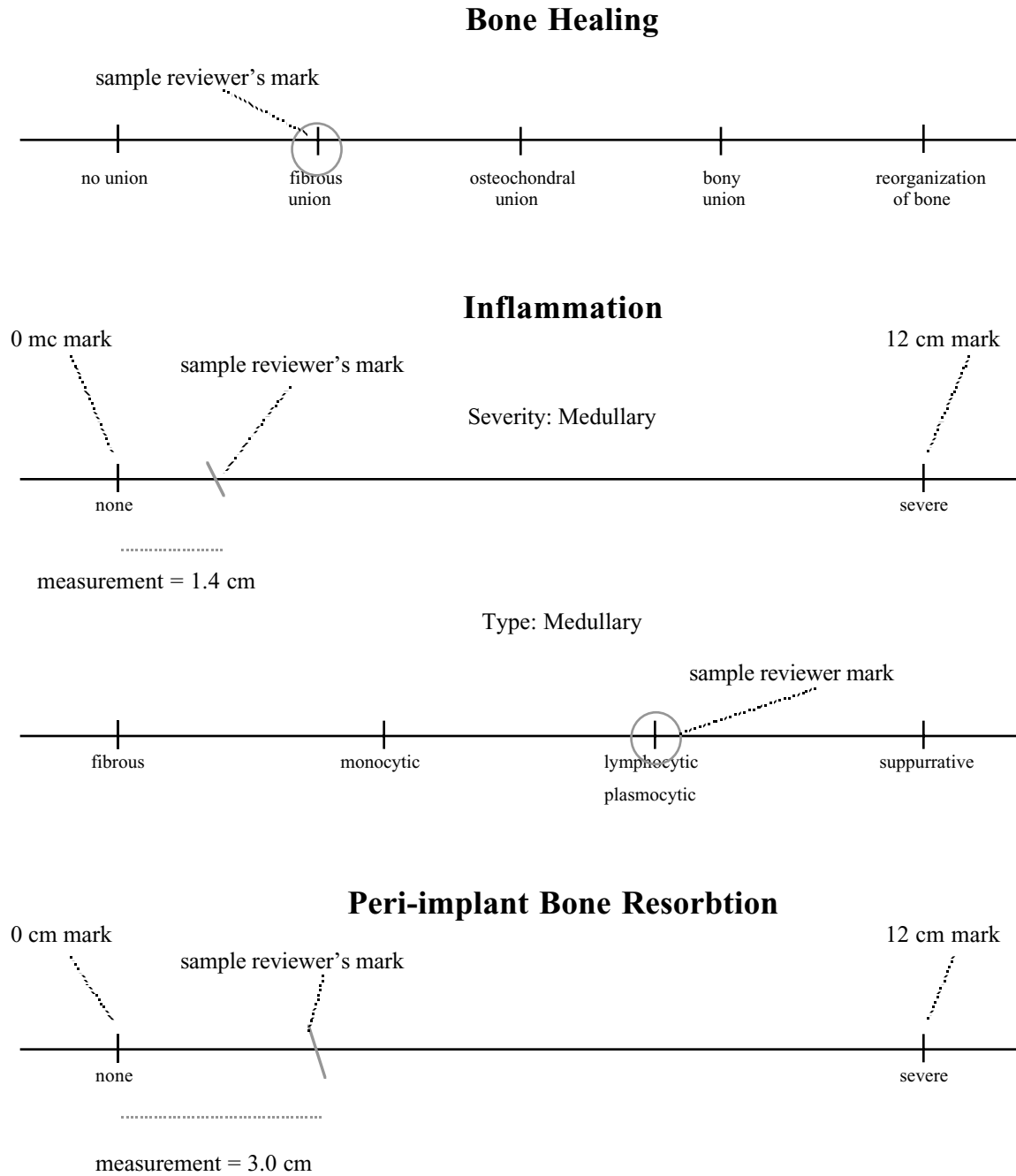
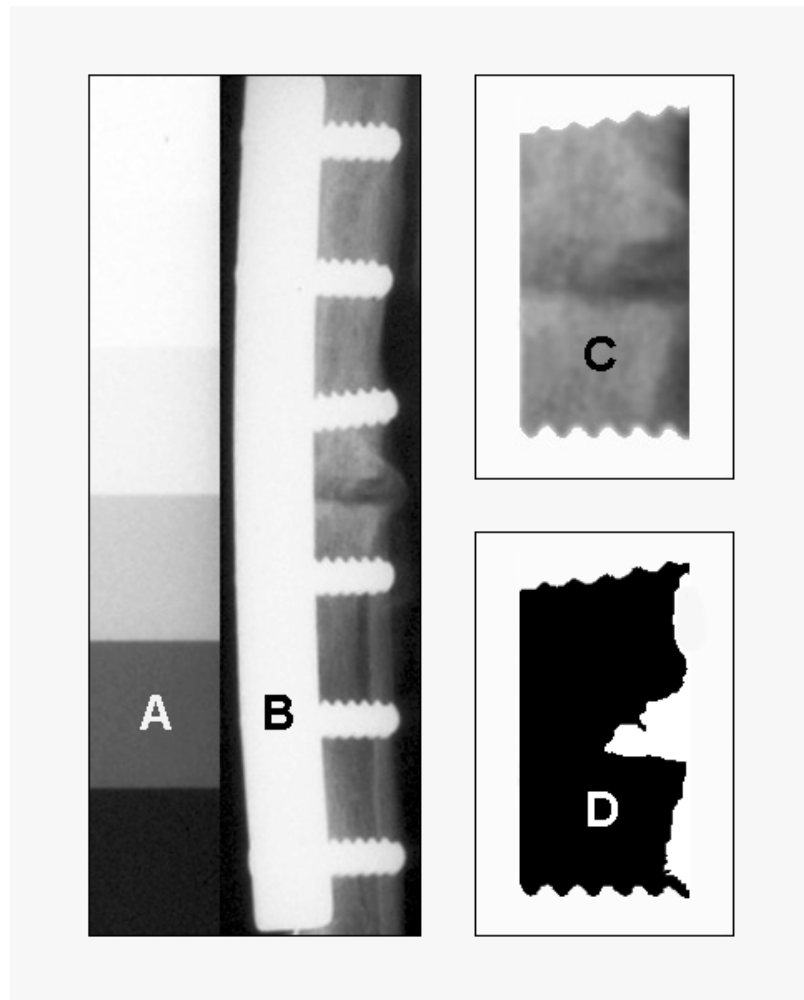


Figure 6

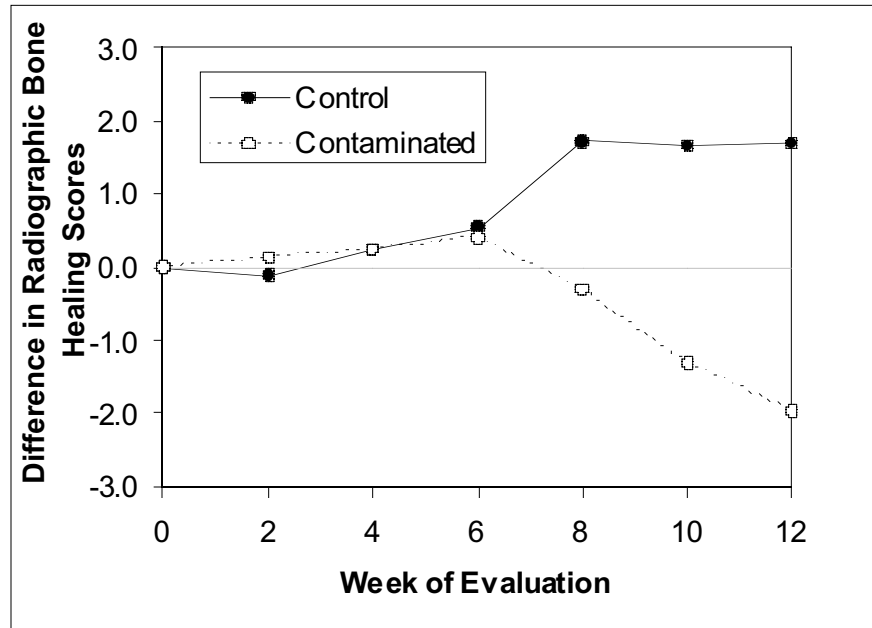
Figure 6: Image Depicting Bone Area Analysis



Digitized image of 8 week post-operative medial-lateral radiograph (Left). Step used as low threshold control (A) plate used as upper threshold limit (B). Magnification of fracture gap area (upper right). Area of analysis depicted (C) with remaining area masked out (white). Binary image of area of analysis after low and high density thresholds have been applied (bottom right). Black area (D) was measured for # of pixel and divided by the # of pixel in the Area of Analysis (C) and then multiplied by 100 to determine Bone Area (BA) at each evaluation.

Figure 7

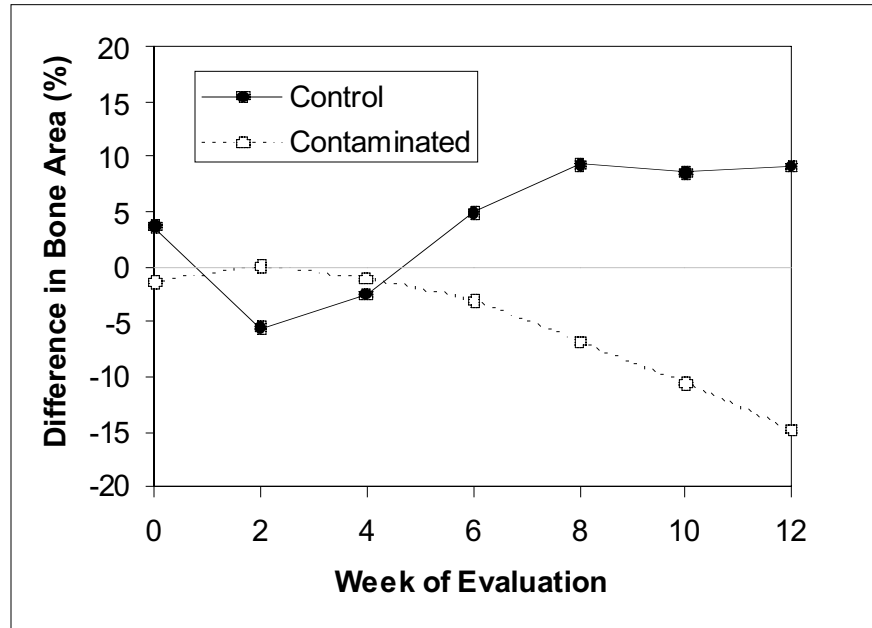
Mean Difference in Bone Area



Mean Difference in Bone Area (DBA) evaluations over time by control (sterile PBS) and contaminated (*S. intermedius*) groups

Figure 8

Mean Difference in Radiographic Bone Healing



Mean Difference in Radiographic Bone Healing (DRBH) evaluations over time by control (sterile PBS) and contaminated (*S. intermedius*) groups.

References

1. Ballin JC. Evaluation of a new topical agent for burn therapy. Silver sulfadiazine (silvadene). *Jama* 1974;230(8):1184-5.
2. Barranco SD, Colmano G. Electrical inhibition of *Staphylococcus aureus*. *Va Med Mon* 1976;103(9):646.
3. Barranco SD, Spadaro JA, Berger TJ, Becker RO. In vitro effect of weak direct current on *Staphylococcus aureus*. *Clin Orthop* 1974;100(0):250-5.
4. Becker RO, Spadaro JA. Treatment of orthopaedic infections with electrically generated silver ions. A preliminary report. *J Bone Joint Surg [Am]* 1978;60(7):871-81.
5. Berger TJ, Spadaro JA, Chapin SE, Becker RO. Electrically generated silver ions: quantitative effects on bacterial and mammalian cells. *Antimicrob Agents Chemother* 1976;9(2):357-8.
6. Bonakdar-pour A, Gaines VD. The radiology of osteomyelitis. *Orthop Clin North Am* 1983;14(1):21-37.
7. Bonewald LF, Mundy GR. Role of transforming growth factor-beta in bone remodeling. *Clin Orthop* 1990(250):261-76.
8. Braden TD. Posttraumatic osteomyelitis. *Vet Clin North Am Small Anim Pract* 1991;21(4):781-811.

9. Braden TD, Johnson CA, Gabel CL, Lott GA, Caywood DD. Posologic evaluation of clindamycin, using a canine model of posttraumatic osteomyelitis. *Am J Vet Res* 1987;48(7):1101-5.
10. Braden TD, Johnson CA, Wakenell P, Tvedten HW, Mostosky UV. Efficacy of clindamycin in the treatment of *Staphylococcus aureus* osteomyelitis in dogs. *J Am Vet Med Assoc* 1988;192(12):1721-1725.
11. Braden TD, Tvedten HW, Mostosky UV, Thomas M, Stickle RL, Kaneene JB. The sensitivity and specificity of radiology and histopathology in the diagnosis of post-traumatic osteomyelitis. *Vet Comp Orthop Traumatol VCOT* 1984;3(2):98-103.
12. Brown SG, Kramers PC. Indirect (secondary) bone healing. In: Bojrab MJ, editor. *Disease mechanisms in small animal surgery*. 2nd ed. Baltimore, Md.: Williams & Wilkins; 1993. p. 671-77.
13. Carter GR, Chengappa MM, Roberts AW. *Essentials of veterinary microbiology*. 5th ed. Baltimore: Williams & Wilkins; 1995.
14. Caywood DD, Wallace LJ, Braden TD. Osteomyelitis in the dog: a review of 67 cases. *J Am Vet Med Assoc* 1978;172(8):943-6.
15. Chakkalakal DA, Lippiello L, Shindell RL, Connolly JF. Electrophysiology of direct current stimulation of fracture healing in canine radius. *IEEE Trans Biomed Eng* 1990;37(11):1048-58.

16. Chandnani VP, Beltran J, Morris CS, Khalil SN, Mueller CF, Burk JM, et al. Acute experimental osteomyelitis and abscesses: detection with MR imaging versus CT [see comments]. *Radiology* 1990;174(1):233-6.
17. Chidgey L, Chakkalakal D, Blotcky A, Connolly JF. Vascular reorganization and return of rigidity in fracture healing. *J Orthop Res* 1986;4(2):173-9.
18. Collinge CA, Goll G, Seligson D, Easley KJ. Pin tract infections: silver vs uncoated pins. *Orthopedics* 1994;17(5):445-8.
19. Colmano G, Edwards SS, Barranco SD. Activated silver coatings for surgical implants. *Va Med* 1979;106(12):928-30.
20. Colmano G, Edwards SS, Barranco SD. Activation of antibacterial silver coatings on surgical implants by direct current: preliminary studies in rabbits. *Am J Vet Res* 1980;41(6):964-6.
21. Costerton JW, Irvin RT, Cheng KJ. The role of bacterial surface structures in pathogenesis. *Crit Rev Microbiol* 1981;8(4):303-38.
22. Darouiche RO, Farmer J, Chaput C, Mansouri M, Saleh G, Landon GC. Anti-infective efficacy of antiseptic-coated intramedullary nails. *J Bone Joint Surg Am* 1998;80(9):1336-40.
23. Davy DT, Connolly JF. The biomechanical behavior of healing canine radii and ribs. *J Biomech* 1982;15(4):235-47.
24. Deyssine M, Rosario E, Isenberg HD. Acute hematogenous osteomyelitis: an experimental model. *Surgery* 1976;79(1):97-9.

25. Difazio MC, MacMahon H, Xu XW, Tsai P, Shiraishi J, Armat o SG, 3rd, et al. Digital chest radiography: effect of temporal subtraction images on detection accuracy. *Radiology* 1997;202(2):447-52.
26. Dorland WAN. *Dorland's Medical dictionary*. 28th ed. Philadelphia, Pa. New York: Saunders Press ;; 1994.
27. Fitzgerald RH, Jr. Experimental osteomyelitis: description of a canine model and the role of depot administration of antibiotics in the prevention and treatment of sepsis. *J Bone Joint Surg [Am]* 1983;65(3):371-80.
28. Fletcher BD, Scoles PV, Nelson AD. Osteomyelitis in children: detection by magnetic resonance. *Work in progress. Radiology* 1984;150(1):57-60.
29. Fossum TW, Hulse DA. Osteomyelitis. *Semin Vet Med Surg (Small Anim)* 1992;7(1):85-97.
30. Fox CL, Jr. Silver sulfadiazine for control of burn wound infections. *Int Surg* 1975;60(5):275-7.
31. Fung LC, Khoury AE, Vas SI, Smith C, Oreopoulos DG, Mittelman MW. Biocompatibility of silver-coated peritoneal dialysis catheter in a porcine model. *Perit Dial Int* 1996;16(4):398-405.
32. Fung MC, Bowen DL. Silver products for medical indications: risk-benefit assessment. *J Toxicol Clin Toxicol* 1996;34(1):119-26.
33. Gillespie WJ, Allardyce RA. Mechanisms of bone degradation in infection: a review of current hypotheses. *Orthopedics* 1990;13(4):407-10.

34. Gristina AG, Costerton JW. Bacterial adherence and the glycocalyx and their role in musculoskeletal infection. *Orthop Clin North Am* 1984;15(3):517-35.
35. Gristina AG, Rovere GD, Shoji H, Nicastro JF. An in vitro study of bacterial response to inert and reactive metals and to methyl methacrylate. *J Biomed Mater Res* 1976;10(2):273-81.
36. Hasuo K, Mizushima A, Mihara F, Hashiguchi N, Murayama S, Uchino A, et al. Intra-arterial digital subtraction angiography with extra-large fields using a computed radiography system in evaluating peripheral vascular disease. *Radiat Med* 1996;14(5):229-33.
37. Hendry AT, Stewart IO. Silver-resistant Enterobacteriaceae from hospital patients. *Can J Microbiol* 1979;25(8):915-21.
38. Herron MR. Osteomyelitis. In: Bojrab MJ, editor. *Disease mechanisms in small animal surgery*. 2nd ed. Philadelphia: Lea & Febiger; 1993. p. 692-96.
39. Hill WR, Pillsbury DM. *Argyria: The Pharmacology of Silver*. Baltimore: Williams & Wilkins; 1939.
40. Hovi I, Hekali P, Korhola O, Valtonen M, Valtonen V, Taavitsainen M, et al. Detection of soft-tissue and skeletal infections with ultra low-field (0.02 T) MR imaging. *Acta Radiol* 1989;30(5):495-9.
41. Hulth A. Current concepts of fracture healing. *Clin Orthop* 1989(249):265-84.
42. Jacob E, Arendt DM, Brook I, Durham LC, Falk MC, Schaberg SJ. Enzyme-linked immunosorbent assay for detection of antibodies to *Staphylococcus aureus* cell walls in experimental osteomyelitis. *J Clin Microbiol* 1985;22(4):547-52.

43. Jang SS, Dorr TE, Biberstein EL, Wong A. Aspergillus deflectus infection in four dogs. *J Med Vet Mycol* 1986;24(2):95-104.
44. Johnson KD, August A, Sciadini MF, Smith C. Evaluation of ground cortical autograft as a bone graft material in a new canine bilateral segmental long bone defect model. *J Orthop Trauma* 1996;10(1):28-36.
45. Lexer E. Experimente uber osteomyelitis. *Arch Klin Chir* 1896;53:266-77.
46. Lexer E. Experimentellen erzeugung osteomyelitischer herde. *Arch Klin Chir* 1894;48:181-200.
47. Mackowiak PA, Jones SR, Smith JW. Diagnostic value of sinus-tract cultures in chronic osteomyelitis. *Jama* 1978;239(26):2772-5.
48. Mader JT. Animal models of osteomyelitis. *Am J Med* 1985;78(6B):213-7.
49. Markel MD, Chao EY. Noninvasive monitoring techniques for quantitative description of callus mineral content and mechanical properties. *Clin Orthop* 1993(293):37-45.
50. Markel MD, Wikenheiser MA, Chao EY. A study of fracture callus material properties: relationship to the torsional strength of bone. *J Orthop Res* 1990;8(6):843-50.
51. Markel MD, Wikenheiser MA, Morin RL, Lewallen DG, Chao EY. The determination of bone fracture properties by dual-energy X-ray absorptiometry and single-photon absorptiometry: a comparative study. *Calcif Tissue Int* 1991;48(6):392-9.

52. Markel MD, Wikenheiser MA, Morin RL, Lewallen DG, Chao EY. Quantification of bone healing. Comparison of QCT, SPA, MRI, and DEXA in dog osteotomies. *Acta Orthop Scand* 1990;61(6):487-98.
53. Marshall JPd, Schneider RP. Systemic argyria secondary to topical silver nitrate. *Arch Dermatol* 1977;113(8):1077-9.
54. Meller Y, Kestenbaum RS, Mozes M, Mozes G, Yagil R, Shany S. Mineral and endocrine metabolism during fracture healing in dogs. *Clin Orthop* 1984(187):289-95.
55. Millis DL, Wilkens BE, Daniel GB, Hubner K, Mathews A, Buonomo FC, et al. Radiographic, densitometric, and biomechanical effects of recombinant canine somatotropin in an unstable osteotomy gap model of bone healing in dogs. *Vet Surg* 1998;27(2):85-93.
56. Nand S, Sengar GK, Jain VK, Gupta TD. Dual use of silver for management of chronic bone infections and infected non-unions. *J Indian Med Assoc* 1996;94(3):91-5.
57. Nickoloff EL, Feldman F, Atherton JV. Bone mineral assessment: new dual-energy CT approach. *Radiology* 1988;168(1):223-8.
58. Norden CW, Kennedy E. Experimental osteomyelitis I. A description of the model. *J Infect Dis* 1970;122:410-18.
59. Paley D, Young MC, Wiley AM, Fornasier VL, Jackson RW. Percutaneous bone marrow grafting of fractures and bony defects. An experimental study in rabbits. *Clin Orthop* 1986(208):300-12.

60. Perren SM. Primary Bone Healing. In: Bojrab MJ, editor. Disease mechanisms in small animal surgery. 2nd ed. Baltimore, Md.: Williams & Wilkins; 1993. p. 663-70.
61. Petty W, Spanier S, Shuster JJ, Silverthorne C. The influence of skeletal implants on incidence of infection. Experiments in a canine model. J Bone Joint Surg [Am] 1985;67(8):1236-44.
62. Piermatti DL, Flo GL. Small animal orthopedics and fracture repair. 3rd ed. Philadelphia, PA: W.B. Saunders Co.; 1997.
63. Prescott RJ, Wells S. Systemic argyria. J Clin Pathol 1994;47(6):556-7.
64. Raptopoulos V, Doherty PW, Goss TP, King MA, Johnson K, Gantz NM. Acute osteomyelitis: advantage of white cell scans in early detection. AJR Am J Roentgenol 1982;139(6):1077-82.
65. Reddy MS, Jeffcoat MK. Digital subtraction radiography. Dent Clin North Am 1993;37(4):553-65.
66. Rissing JP. Animal models of osteomyelitis. Knowledge, hypothesis, and speculation. Infect Dis Clin North Am. 1990;4(3):377-90. Review.
67. Rissing JP, Buxton TB, Fisher J, Harris R, Shockley RK. Arachidonic acid facilitates experimental chronic osteomyelitis in rats. Infect Immun 1985;49(1):141-4.
68. Rodet A. Physiologie pathologique-etude experimentale sur l'osteomyelite. CR Acad Sci 1885;99:569-71.

69. Rudd RG. A rational approach to the diagnosis and treatment of osteomyelitis. *Comp Cont Edu* 1986;8(4):225-32.
70. Scheman L, Janota M, Lewin P. The production of experimental osteomyelitis. *JAMA* 1941;117:1525-29.
71. Sciadini MF, Dawson JM, Johnson KD. Bovine-derived bone protein as a bone graft substitute in a canine segmental defect model. *J Orthop Trauma* 1997;11(7):496-508.
72. Scott DW, Miller WH, Griffin CE. Bacterial Skin Diseases. In: Muller GH, Kirk RW, editors. *Muller and Kirk's small animal dermatology*. 5th / ed. Philadelphia: W.B. Saunder Co.; 1995. p. 280-281.
73. Shinogi M, Maeizumi S. Effect of preinduction of metallothionein on tissue distribution of silver and hepatic lipid peroxidation. *Biol Pharm Bull* 1993;16(4):372-4.
74. Simmons DJ. Fracture healing perspectives. *Clin Orthop* 1985(200):100-13.
75. Sinibaldi KR, Pugh J, Rosen H, Liu SK. Osteomyelitis and neoplasia associated with use of the Jonas intramedullary splint in small animals. *J Am Vet Med Assoc* 1982;181(9):885-90.
76. Smith CW, G. SA, Smith AR, Dorner JL. Osteomyelitis in the Dog: A Retrospective Study. *J Am Anim Hosp Assoc* 1978;14:589-592.
77. Smith MM. Orthopedic Infections. In: Slatter DH, editor. *Textbook of small animal surgery*. 2nd ed. Philadelphia: W.B. Saunders; 1993. p. 1685-94.

78. Smith MM, Vasseur PB, Saunders HM. Bacterial growth associated with metallic implants in dogs. *J Am Vet Med Assoc* 1989;195(6):765-767.
79. Spadaro JA. Bone formation and bacterial inhibition with silver and other electrodes. *Reconstr Surg Traumatol* 1985;19:40-50.
80. Spadaro JA, Berger TJ, Barranco SD. Antibacterial effects of silver electrodes with weak direct current. *Agents in Chemotherapy* 1974;6:637-42.
81. Spadaro JA, Chase SE, Webster DA. Bacterial inhibition by electrical activation of percutaneous silver implants. *J Biomed Mater Res* 1986;20(5):565-77.
82. Stead AC. Osteomyelitis in the dog and cat. *J Small Anim Pract* 1984;25:1-13.
83. Stevenson S, Olmstead ML, Kowalski J. Bacterial culturing for prediction of postoperative complications following open fracture repair in small animals. *Veterinary Surgery* 1986;15(1):99-102.
84. Teague HD, Alsaker R, Braden TD, Caywood DD. Two cases of foreign-body osteomyelitis secondary to retained surgical sponges. *Vet Med Small Anim Clin* 1978;73(10):1279-86.
85. Webster DA, Spadaro JA, Becker RO, Kramer S. Silver anode treatment of chronic osteomyelitis. *Clin Orthop* 1981(161):105-14.
86. Westhofen M, Schafer H. Generalized argyrosis in man: neurotological, ultrastructural and X-ray microanalytical findings. *Arch Otorhinolaryngol* 1986;243(4):260-4.
87. Wheat J. Diagnostic strategies in osteomyelitis. *Am J Med* 1985;78(6B):218-24.

88. Wilkens BE, Millis DL, Daniel GB, Munson L, Patel KR, Buonomo FC.
Metabolic and histologic effects of recombinant canine somatotropin on bone healing in dogs, using an unstable osteotomy gap model. *Am J Vet Res* 1996;57(9):1395-401.
89. Wolf AM. Histoplasma capsulatum osteomyelitis in the cat. *J Vet Intern Med* 1987;1(4):158-62.

Vita

Russell Eric Wright was born on January 21, 1968 in Daly City, California, son of Gilbert and Josephine Wright. Eric attended Northgate High School prior to attending the University of California at Santa Barbara in 1986. He graduated with a Bachelor of Arts degrees in Biologic Sciences with an emphasis in Microbiology. He worked in the quality assurance division of Ortho Diagnostics Inc. for one year post undergraduate. He attended Colorado State University School of Veterinary Medicine, where he graduated as a Doctor of Veterinary Medicine in 1995.

Eric completed a small animal internship in small animal medicine and surgery at Southwest Veterinary Specialist in Tucson, Arizona in 1996. He finished a residency in small animal surgery at the Virginia-Maryland School of Veterinary Medicine on July 1, 1999.

After finishing his Masters of Science in Veterinary Medical Sciences at the VMRCVM, Eric plans to return to Santa Barbara, California to begin a small animal surgical referral practice.